Parameterization for Cloud Longwave Scattering for Use in Atmospheric Models

MING-DAH CHOU

Laboratory for Atmospheres, NASA/Goddard Space Flight Center, Greenbelt, Maryland

KYU-TAE LEE

Department of Atmospheric and Environmental Science, Kangnung National University, Kangnung, South Korea

SI-CHEE TSAY

Laboratory for Atmospheres, NASA/Goddard Space Flight Center, Greenbelt, Maryland

QIANG FU

Atmospheric Science Program, Department of Oceanography, Dalhousie University, Halifax, Nova Scotia, Canada

(Manuscript received 9 June 1997, in final form 10 February 1998)

ABSTRACT

A parameterization for the scattering of thermal infrared (longwave) radiation by clouds has been developed based on discrete-ordinate multiple-scattering calculations. The effect of backscattering is folded into the emission of an atmospheric layer and the absorption between levels by scaling the cloud optical thickness. The scaling is a function of the single-scattering albedo and asymmetry factor. For wide ranges of cloud particle size, optical thickness, height, and atmospheric conditions, flux errors induced by the parameterization are small. They are <4 W m^{-2} (2%) in the upward flux at the top of the atmosphere and <2 W m^{-2} (1%) in the downward flux at the surface. Compared to the case that scattering by clouds is neglected, the flux errors are more than a factor of 2 smaller. The maximum error in cooling rate is $\approx$8%, which occurs at the top of clouds, as well as at the base of high clouds where the difference between the cloud and surface temperatures is large.

With the scaling approximation, radiative transfer equations for a cloudy atmosphere are identical with those for a clear atmosphere, and the difficulties in applying a multiple-scattering algorithm to a partly cloudy atmosphere (assuming homogeneous clouds) are avoided. The computational efficiency is practically the same as that for a clear atmosphere. The parameterization represents a significant reduction in one source of the errors involved in the calculation of longwave cooling in cloudy atmospheres.

1. Introduction

Scattering of solar radiation by clouds is well recognized as a dominant factor affecting the earth's planetary albedo and, hence, the climate. However, scattering of thermal infrared (longwave, or LW) radiation by clouds are commonly neglected in weather and climate studies for two reasons: 1) Except in the 10-μm window region, LW radiative transfer in clouds is dominated by the absorption due to water vapor and water/ice particles. The effect of scattering is relatively week. 2) Multiple-scattering calculations in atmospheric models require a great amount of computing time, especially when there are multiple partly cloudy layers.

Only until recently, the effect of scattering of LW radiation by clouds on the atmospheric cooling rate and the heating at the surface has been studied with detailed multiple-scattering calculations. Fu et al. (1997) used a discrete-ordinate multiple-scattering scheme to study the effect of scattering by clouds on the fluxes at the top of the atmosphere and at the surface, as well as the atmospheric cooling rate. They also compared the accuracy and computing speed of the scattering scheme with different discrete-ordinate streams and found that a combined δ-two-stream and δ-four-stream approximations are suitable for efficient implementation in a general circulation model (GCM) for climate studies. In a study on the spectral LW cooling in cloud computed with multiple-scattering radiation codes, O'Brien et al. (1997) found that neglecting the LW scattering in clouds leads to significant errors in the atmospheric window between 800 and 1250 cm^{-1}.

Nearly all multiple-scattering schemes developed for

Corresponding author address: Dr. Ming-Dah Chou, Code 913, Laboratory for Atmospheres, NASA/Goddard Space Flight Center, Greenbelt, MD 20771.
E-mail: chou@climate.gsfc.nasa.gov

weather and climate studies apply only to plane-parallel (horizontally homogeneous) atmospheres; they cannot be applied directly to partly cloudy atmospheres. Efficient scattering algorithms for application to a horizontally nonhomogeneous atmosphere are not yet available. In a GCM, it is common that calculations of LW radiative terms take >30% of the total computing time. To include calculations of scattering of LW radiation in a partly cloudy atmosphere, it will require either smearing of a partly cloudy layer and reducing it to an equivalent homogeneous layer or dividing the atmosphere into homogenous sections. The former approach will degrade the accuracy of radiation calculations, while the latter approach will greatly enhance the computing time. Therefore, it is highly desirable to avoid explicit calculations of multiple-scattering in the thermal infrared (IR) in climate studies and, at the same time, retain the accuracy of flux calculations. In this study, we develop a simple parameterization for the scattering of LW radiation by clouds, which can be implemented in long-term GCM climate simulations without requiring explicit calculations of multiple scattering. In addition to enhancing the accuracy, this parameterization practically requires no extra computing time as compared to a pure absorbing/emitting atmosphere. The radiative transfer calculations in this study are one-dimensional, only in the vertical direction. We address neither the emission/scattering on the sides of clouds nor the effect of horizontal inhomogeneity in clouds. These problems are very complicated (e.g., Harshvardhan and Weinman 1982; Killen and Ellingson 1994; Cahalan et al. 1994) and are beyond the scope of this study.

2. Cloud optical properties and the radiative transfer model

The effect of clouds on LW scattering is studied here for spherical liquid water droplets and randomly oriented hexagonal ice crystals. The important parameters of cloud droplets in radiative transfer is the extinction coefficient, single-scattering albedo, and scattering phase function (or asymmetry factor). For water droplets, these parameters are computed using the Mie scattering algorithm assuming a modified gamma function for the size distribution. For ice crystals, they are computed using the method of Fu et al. (1998), which employs a linear combination of single-scattering properties derived from the Mie theory, the anomalous diffraction theory, and the geometric optics method. A total of 28 cirrus particle size distributions from aircraft measurements are used. Figures 1 and 2 show the distributions of the extinction coefficient, asymmetry factor, and single scattering co-albedo in the LW spectral region. Results shown in Fig. 1 are for various particle size distributions with the mass-weighted effective mean particle radius for water cloud, r_w, equal to 4, 8, and 16 μm, and the results shown in Fig. 2 are for two cirrus cloud samples with the geometric mean particle size, r_i as defined in Fu (1996), of 50 and 95 μm. Generally, the extinction coefficient decreases with increasing r_e (Figs. 1a and 2a), whereas the asymmetry factor increases with increasing r_e (Figs. 1b and 2b), where r_e denotes r_w for water droplets and r_i for ice crystals. For the single scattering co-albedo (Figs. 1c and 2c), it decreases with increasing r_e for $\nu > 1000$ cm^{-1}, where ν is the wavenumber.

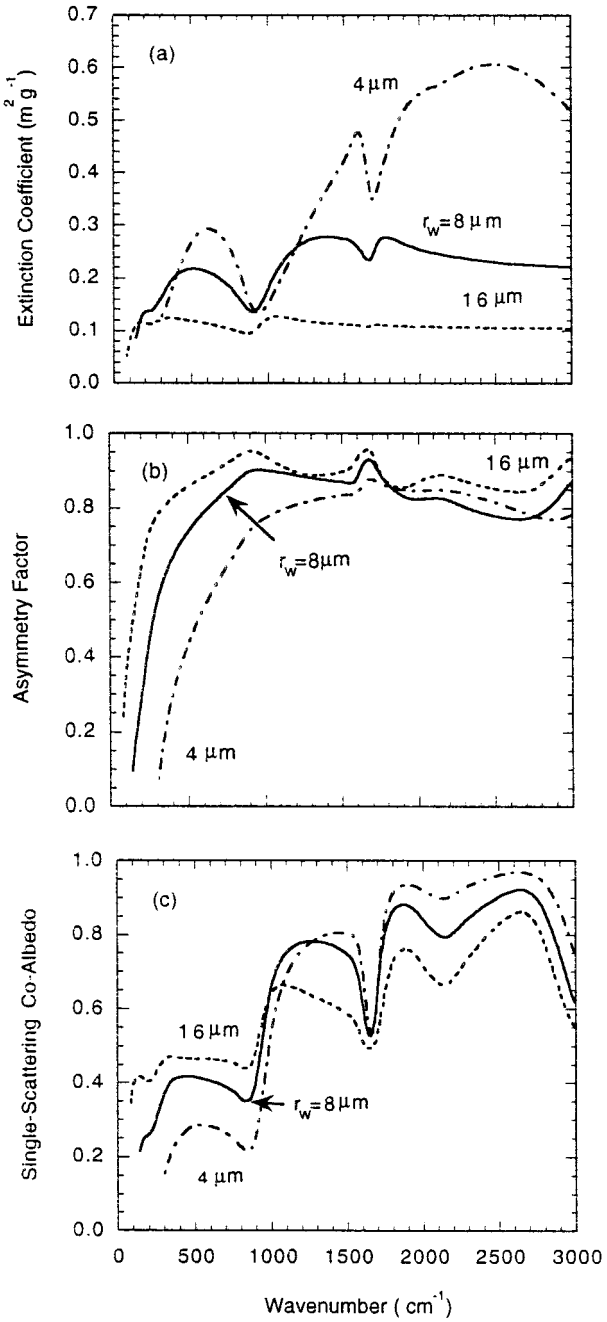

FIG. 1. Spectral distributions of (a) the extinction coefficient, (b) asymmetry factor, and (c) single scattering co-albedo of liquid water cloud droplets. Here, r_w is the mass-weighted effective mean particle radius.

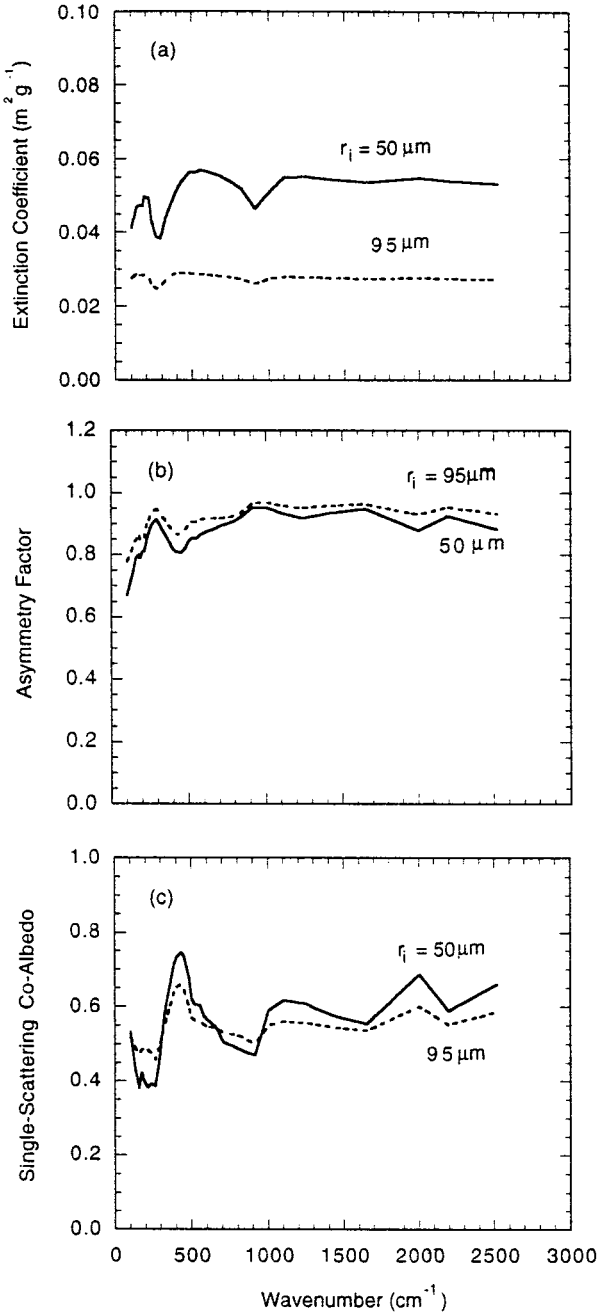

FIG. 2. Same as Fig. 1, except for two cirrus cloud samples with the generalized effective particle size, r_i, equal to 50 and 95 μm, respectively.

We use the discrete-ordinate algorithm developed by Stamnes et al. (1988) to explicitly include the LW scattering in flux calculations. When scattering by clouds is either excluded or parameterized, we use the LW radiation scheme of Chou et al. (1993) and Chou and Suarez (1994) to compute fluxes. This scheme has been implemented in the GEOS (Goddard Earth Observing System) GCM (Schubert et al. 1993), and the Goddard Cloud Ensemble Model (Tao et al. 1996). In this radiation scheme, there are two options for computing transmission functions. One option is to use the *k*-distribution approximation across the entire IR spectrum except the 9.6-μm O_3 band, where *k* is the gaseous absorption coefficient. This *k*-distribution approximation is different from the commonly used correlated *k*-distribution approximation in that the effect of pressure and temperature on absorption is taken into account by scaling the absorption coefficient with a simple function linear in pressure and quadratic in temperature. Fluxes and cooling rate computed using this option are very accurate below the 20-mb level but are not as accurate above this level. Since the purpose of this study is to investigate and parameterize the effect of cloud scattering on LW radiation, radiative transfer calculations above the 20-mb level are not important. For the 9.6-μm O_3 band, the band-averaged flux transmission function is interpolated from precomputed transmission tables, which cannot be applied to multiple-scattering algorithms in a cloudy atmosphere for flux calculations. Therefore, the absorption due to O_3 is not included. Furthermore, the trace gases such as N_2O, CH_4, and CFCs are deleted from the LW radiation scheme to simplify the calculations. These simplifications should not impact the results and conclusions of this study.

The IR spectrum is divided into 10 spectral bands, three of them are in the 15-μm CO_2 band (Chou et al. 1993). A maximum of six values of *k*, or equivalently six ranges of the *k*-distribution function, are used in computing the band-averaged flux transmittance in each spectral band,

$$T_f(u) = \sum_{i=1}^{6} w_i e^{-uk_i/\overline{\mu}}, \tag{1}$$

where *u* is the pressure- and temperature-scaled absorber amount, *w* is the k-distribution function (or the weight), and $1/\overline{\mu}$ is the diffusivity factor that converts the absorption coefficient to an equivalent absorption coefficient for flux transmittance. It is approximated by 1.66. Sets of *k* were prespecified and that of *w* are precomputed for each band. Based on (1), fluxes, F_i, are computed for each absorption coefficient k_i, and the total flux is computed from

$$F = \sum_{i=1}^{6} w_i F_i. \tag{2}$$

Mean values of the extinction coefficient, β, single scattering albedo, ω, and asymmetry factor, *g*, are derived for each spectral band from

$$\beta(r_e) = \sum_{\Delta\nu} \beta_\nu(r_e) B_\nu(\theta_o) \Big/ \sum_{\Delta\nu} B_\nu(\theta_o), \tag{3}$$

$$\omega(r_e) = \sum_{\Delta\nu} \omega_\nu(r_e)\beta_\nu(r_e) B_\nu(\theta_o) \Big/ \sum_{\Delta\nu} \beta_\nu(r_e) B_\nu(\theta_o), \tag{4}$$

and

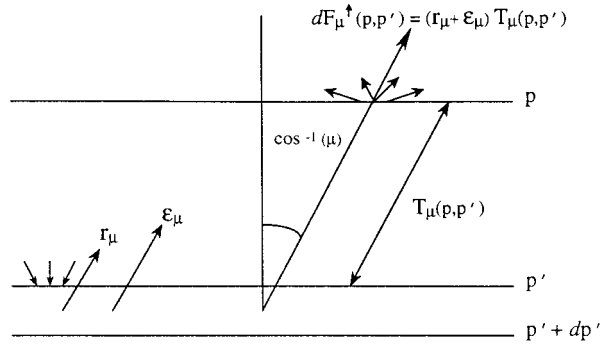

FIG. 3. The contribution of a layer dp' to the upward radiation at p.

$$g(r_e) = \sum_{\Delta\nu} g_\nu(r_e)\omega_\nu(r_e)\beta_\nu(r_e)B_\nu(\theta_o)/ \sum_{\Delta\nu} \omega_\nu(r_e)\beta_\nu(r_e)B_\nu(\theta_o), \quad (5)$$

where B is the Planck function, θ_o is the medium value of the atmospheric temperature set to be 250 K, and $\Delta\nu$ is the spectral interval of a band.

Fluxes and cooling rates are computed for the midlatitude summer and the subarctic winter atmospheres taken from Anderson et al. (1986). Clouds are set at three heights: 200–275 mb for high clouds, 500–575 mb for middle clouds, and 800–875 mb for low clouds. It is assumed that the high clouds contain ice crystals and the middle and low clouds contain liquid droplets. Various cloud optical thickness are used in the flux calculations. The optical thickness in the visible spectral region, τ_{vis} ranges from 0.5 to 20. These values are extrapolated to the LW spectral region according to detailed calculations of the spectral extinction coefficient. The atmospheres are divided into 75 layers. The thickness of a layer below the 100-mb level is ≈25 mb.

3. Scaling of cloud optical thickness

Let us consider the contribution of a layer dp' to the upward radiation at p (Fig. 3). The layer emits (ε_μ) and reflects (r_μ) radiation in the direction μ, which are the sources of the radiation. We consider ε_μ and r_μ as the sources of the radiation since they would not exist without the layer dp'. The source radiation is absorbed and reflected by the atmosphere between p and p'. When the radiation emerges from p, $dF_\mu{\uparrow}(p, p')$, it consists of directly transmitted radiation and upward scattered radiation.

At a given wavenumber, the radiation emitted by the layer dp' in the direction μ is

$$\varepsilon_\mu = [(1 - \omega(p')]B(p')d\tau(p')/\mu, \quad (6)$$

where B is the Planck function, τ is the optical thickness, μ is the cosine of the zenith angle of a radiation beam, and ω is the single-scattering albedo given by

$$\omega = d\tau_s/(d\tau_a + d\tau_s) = d\tau_s/d\tau, \quad (7)$$

τ_s and τ_a are the optical thickness for scattering and absorption, respectively. All the optical properties are wavenumber dependent, which is not explicitly expressed in the equations.

The radiation reflected by the layer dp' in the direction μ is

$$r_\mu = \left[\frac{1}{2}\int_{-1}^{0} I_{\mu'}(p')P(\mu, \mu')\, d\mu'\right][\omega(p')d\tau(p')/\mu], \quad (8)$$

where I is the incident radiance and $P(\mu, \mu')$ is the scattering phase function. For incident radiation from above, μ' is negative.

If we assume the incident radiance is isotropic and replace the term in the first bracket of (8) by a mean over μ, we have

$$r_\mu = b(p')\omega(p')I(p')d\tau(p')/\mu, \quad (9)$$

where b is the mean fraction of the radiation scattered in the upward direction for isotropic radiation incident from above,

$$b = \frac{1}{2}\int_0^1 d\mu \int_{-1}^{0} P(\mu, \mu')\, d\mu'. \quad (10)$$

It is noted that the approximation of (8) by (9) will have a significant effect on radiance calculations, but is expected to have little effect on flux calculations when averaged over μ. Assuming that the scattering phase function can be approximated by the Henyen–Greenstein function, the backscattering function b is computed as a function of the asymmetry factor g and fit by a polynomial function

$$b = 1 - \sum_{i=1}^{4} a_i g^{i-1}, \quad (11)$$

where $a_1 = 0.5$, $a_2 = 0.3738$, $a_3 = 0.0076$, and $a_4 = 0.1186$.

If we further approximate $I(p')$ by $B(p')$, the *apparent* emission of the layer, dp', reduces to

$$\varepsilon'_\mu = \varepsilon_\mu + r_\mu = [1 - \omega(p')f(p')]B(p')d\tau(p')/\mu, \quad (12)$$

where $f = 1 - b$ is the fraction of radiation scattered downward (upward) for radiation incident from above (below).

Since the tropospheric temperature decreases with increasing height, the radiance I incident from above (below) is smaller (greater) than B. The atmosphere is more opaque closer to the surface, and the difference between I and B decreases with decreasing height. It is, therefore, expected that the error introduced in the *apparent* emission by using (12) is smaller for lower clouds.

For computing the transmittance between p and p', we need to consider the radiation both absorbed and downward-scattered. The optical thickness of a layer dp associated with the former is $d\tau_a$ and that with the latter is $(1 - f)d\tau_s$. Therefore, the *apparent* optical thickness for the extinction can be approximated by

$$d\tilde{\tau} = [d\tau_a + (1 - f)d\tau_s] = (1 - \omega f)d\tau, \quad (13)$$

and the transmittance between p and p' can be written as

$$T_\mu(p, p') = \exp\left[-\frac{1}{\mu}\int_p^{p'} [1 - \omega(p'')f(p'')]\frac{\partial\tau(p, p'')}{\partial p''}\, dp''\right]. \quad (14)$$

From (12)–(14), the contribution of the layer dp' to the upward flux at p is

$$dF_\mu\uparrow(p, p') = [B(p')d\tilde{\tau}(p')/\mu] \times \exp\left\{-\frac{1}{\mu}\int_p^{p'}\left[\frac{\partial}{\partial p''}\tilde{\tau}(p, p'')\right] dp''\right\}. \quad (15)$$

By vertical integration, we have

$$F_\mu\uparrow(p) = B_s T_\mu(p, p_s) + \int_{p_s}^{p} B(p')\left[\frac{\partial}{\partial p'}T_\mu(p, p')\right] dp', \quad (16)$$

where B_s is the Planck function at the earth's surface temperature. Integration over angles, the upward flux can be computed from

$$F\uparrow(p) = \pi B_s T(p, p_s) + \int_{p_s}^{p} \pi B(p')\left[\frac{\partial}{\partial p'}T(p,p')\right] dp', \quad (17)$$

where $T(p, p')$ is the flux transmittance given by

$$T(p, p') = 2\int_0^1 T_\mu(p, p')\mu\, d\mu. \quad (18)$$

Similarly, the total downward flux can be computed from

$$F\downarrow(p) = \int_0^{p} \pi B(p')\left[\frac{\partial}{\partial p'}T(p, p')\right] dp'. \quad (19)$$

Equations (17) and (19) are identical to that without scattering (i.e., $\tau_s = 0$), except the optical thickness is scaled by (13). Integration of (17) and (19) over the spectrum gives us total fluxes.

It is noted that when scattering is neglected, we have $f = 1$, and the optical thickness and transmittance reduce to

$$d\tilde{\tau} = (1 - \omega)d\tau \quad (20)$$

and

$$T_\mu(p, p') = \exp\left\{-\frac{1}{\mu}\int_p^{p'} [1 - \omega(p'')]\frac{\partial\tau(p, p'')}{\partial p''}\, dp''\right\}. \quad (21)$$

Thus, the transmittance is smaller for the case that scattering is included, Eq. (14), than the case that scattering is neglected, Eq. (21). This is equivalent to the situation of a more opaque atmosphere for the former case than the latter case. Therefore, we can expect that the upward (downward) flux for the former case is smaller (larger) than the latter case. Numerical results are shown in the following section.

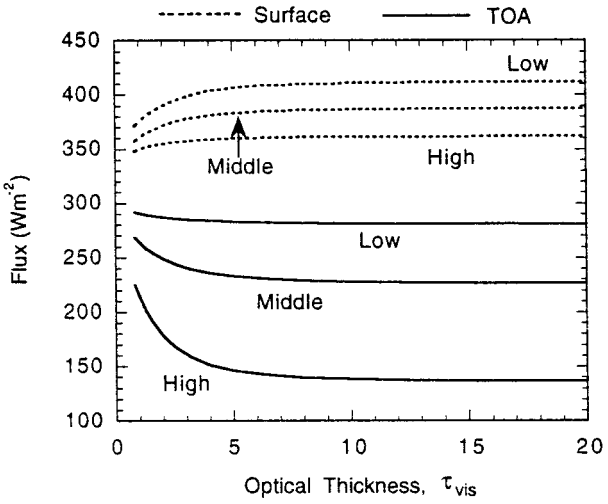

FIG. 4. The upward flux at the TOA and the downward flux at the surface calculated for $r_i = 50$ μm for the high cloud and $r_w = 8$ μm for the middle and low clouds. Here, τ_{vis} is the cloud optical thickness in the visible spectral region. Calculations are for the midlatitude summer atmosphere.

4. Results

Figure 4 shows the upward flux at the top of the atmosphere (TOA) and the downward flux at the surface as a function of the cloud optical thickness in the visible spectral region, τ_{vis}. Fluxes are calculated for the midlatitude summer atmosphere using the six-stream discrete-ordinate scattering algorithm with scattering properly included. Results are shown for the high ($r_i = 50$ μm), middle ($r_w = 8$ μm), and low ($r_w = 8$ μm) cloud cases. The cloud optical thickness in the IR bands is computed by scaling $\tau_{vis}(r_e)$ with a factor $R = \beta_{ir}(r_e)/\beta_{vis}(r_e)$, which varies with spectral bands. As a reference, the value of R for the band located in 800–980 cm^{-1} is 1.02 for $r_i = 50$ μm and 0.74 for $r_w = 8$ μm. The TOA flux decreases with increasing τ_{vis}, but the downward surface flux increases with increasing τ_{vis}. This is expected as the atmospheric temperature decreases with height, and a more opaque cloud has the effects of reducing the TOA flux and enhancing the downward surface flux.

Figure 5 shows errors in the TOA and surface fluxes. In computing fluxes using Eq. (17), the vertical integration is calculated from

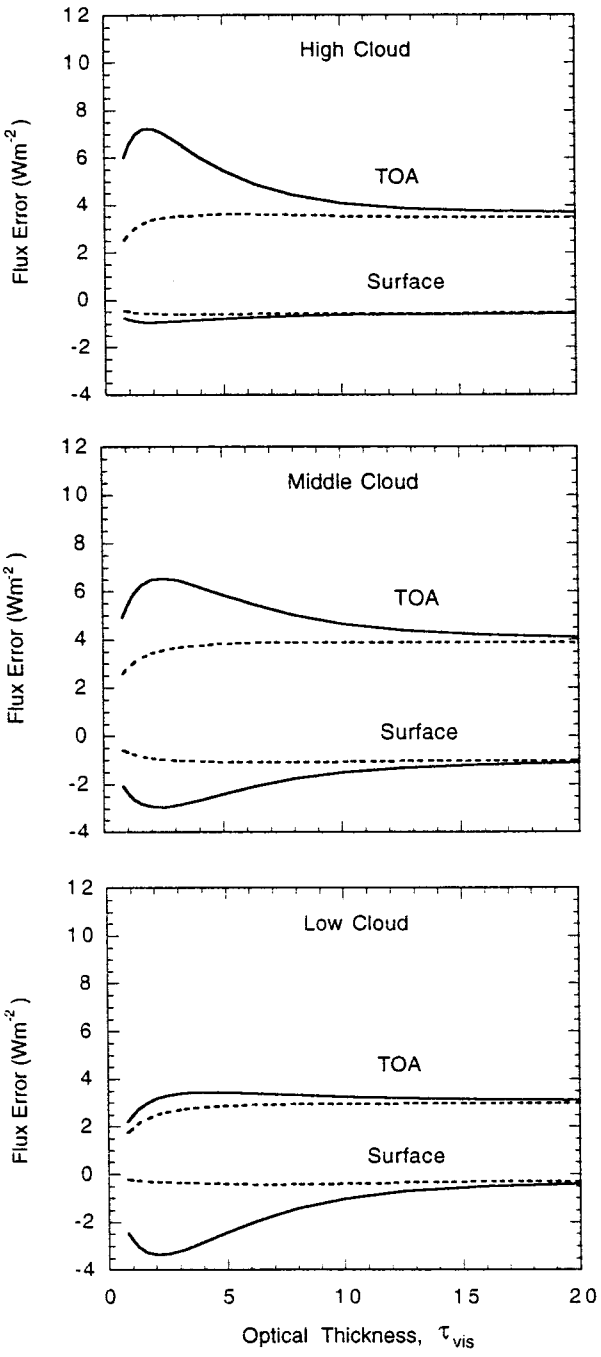

FIG. 5. Errors in the TOA and surface fluxes for high, middle, and low clouds. The solid curves are for the case that scattering is neglected, and the dashed curves are for the parameterization that the cloud optical thickness is scaled by $(1 - \omega f)$. The effective mean particle sizes used are $r_w = 50$ μm for the high cloud and $r_w = 8$ μm for the middle and low clouds. Calculations are for the midlatitude summer atmosphere.

$$\int \pi B(p')\left[\frac{\partial}{\partial p'}T(p, p')\right] dp' = \sum \pi B(p' + 0.5\Delta p)[T(p, p') - T(p, p' + \Delta p)],$$

where Δp is the thickness of a layer. The solid curves are for the case that scattering is neglected, Eq. (20), and the dashed curves are for the parameterization, Eq. (13). In both cases, fluxes are overestimated at the TOA and underestimated at the surface. The upward flux at the top of a cloud layer can be expressed symbolically as

$$F\uparrow = F_a\uparrow + \Delta F\uparrow - \Delta F\downarrow, \tag{22}$$

where F is the flux when scattering is included, F_a is the flux when scattering is neglected, $\Delta F\uparrow$ is the backward-scattering of the radiation incident from above, and $\Delta F\downarrow$ is the backward-scattering of the radiation incident from below. The last two components are the effects due to scattering. The overestimation of the TOA fluxes for the case without cloud scattering as shown by the solid curves indicates that $\Delta F\downarrow > \Delta F\uparrow$. This is a result primarily of the fact that, at a given pressure level, the upward flux is larger than the downward flux, leading to a larger downward backscattered flux than the upward backscattered flux. Similarly, the downward flux at the base of a cloud layer can be expressed as

$$F\downarrow = F_a\downarrow + \Delta F\downarrow - \Delta F\uparrow. \tag{23}$$

The underestimation of the surface fluxes for the case without cloud scattering as shown in the figure also indicates that $\Delta F\downarrow > \Delta F\uparrow$. Both errors in the TOA and surface fluxes induced by neglecting scattering attain a maximum at $\tau_{vis} \approx 2$. The maximum error in the TOA flux is $\approx$8 W m^{-2}. It occurs in the high cloud case where the transmittance between TOA and the cloud top is larger than that for the lower cloud cases. The maximum error in the downward surface flux is $\approx$3.5 W m^{-2}, which occurs in the low cloud case where the transmittance between the cloud base and the surface is larger than that for the higher cloud cases.

When the effect of scattering is included by scaling the optical thickness using (13), the transmittance is given by (14), which is smaller than the transmittance given by (21) without including the scattering effect. The atmosphere is therefore more opaque in the former case than in the latter case. Therefore, the TOA flux is smaller and the downward surface flux is larger in the former case than in the latter case. It can be seen from Fig. 5 that the overestimation of TOA flux and the underestimation of surface flux with scattering neglected (solid curves) are significantly reduced when the simple scaling of the cloud optical thickness of (13) is applied (dashed curves), especially for $\tau_{vis} < 8$. For a large cloud optical thickness, the values of $\tilde{\tau}$ computed from (13) and (20) are both large, and the transmittances computed from (14) and (21) are both small. Therefore, the difference in fluxes between the cases with scattering neglected and with the parameterization is very small.

When different atmospheres and r_e are used, results are similar to that shown in Fig. 5. Figure 6 shows flux errors for the same particle size as that shown in Fig. 5 but the subarctic winter atmosphere is used, whereas

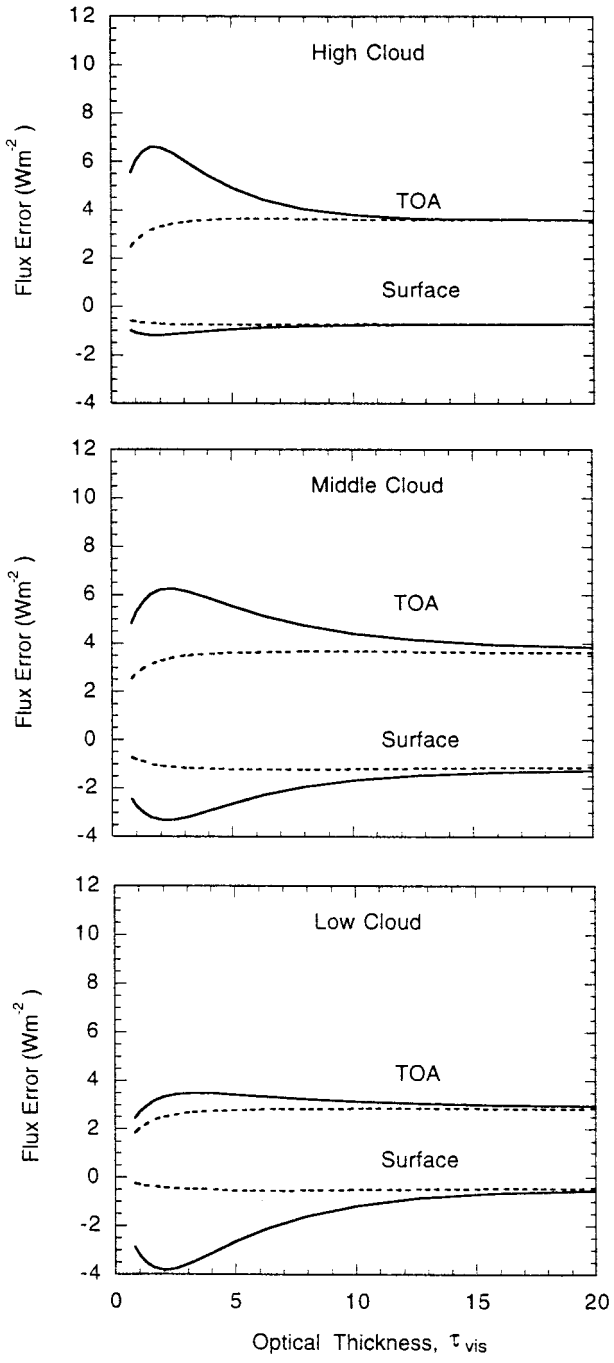

FIG. 6. Flux errors for the same particle sizes as that shown in Fig. 5, except the subarctic winter atmosphere is used.

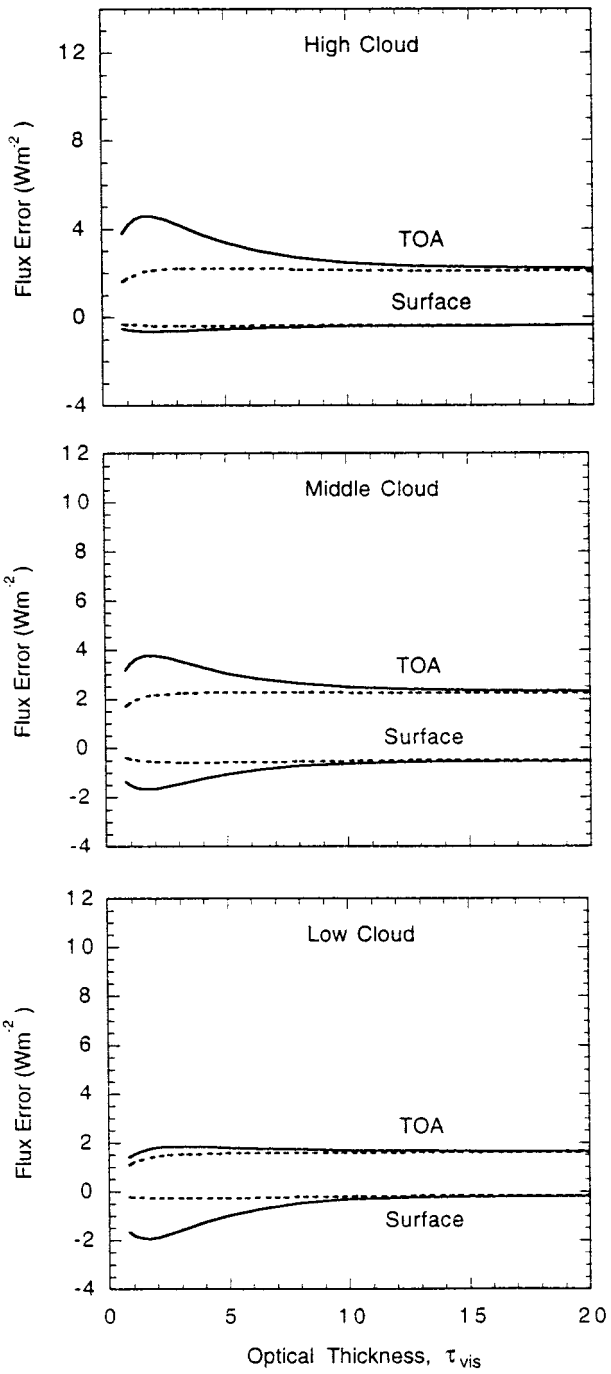

FIG. 7. The flux errors for the same midlatitude summer atmosphere as in Fig. 5, except for $r_w = 95$ μm for the high cloud and $r_w = 16$ μm for the middle and low clouds.

Fig. 7 shows flux errors for the same midlatitude summer atmosphere but the particle sizes are $r_i = 95$ μm for the high cloud and $r_w = 16$ μm for the middle and low clouds. It can be seen that the patterns of the flux errors are all similar with only a small difference in magnitude.

Cooling rate profiles for the midlatitude summer atmosphere with $r_i = 50$ μm for the high cloud and $r_w = 8$ μm for the middle and low clouds are shown in Fig. 8. Scattering by cloud particles is properly included in the flux calculations by using a six-stream discrete-ordinate scattering algorithm. Results are shown for three cloud optical thicknesses in the visible spectral region, $\tau_{vis} = 1$, 5, and 25. Clouds are 75 mb thick and are divided into three layers with a thickness of 25 mb

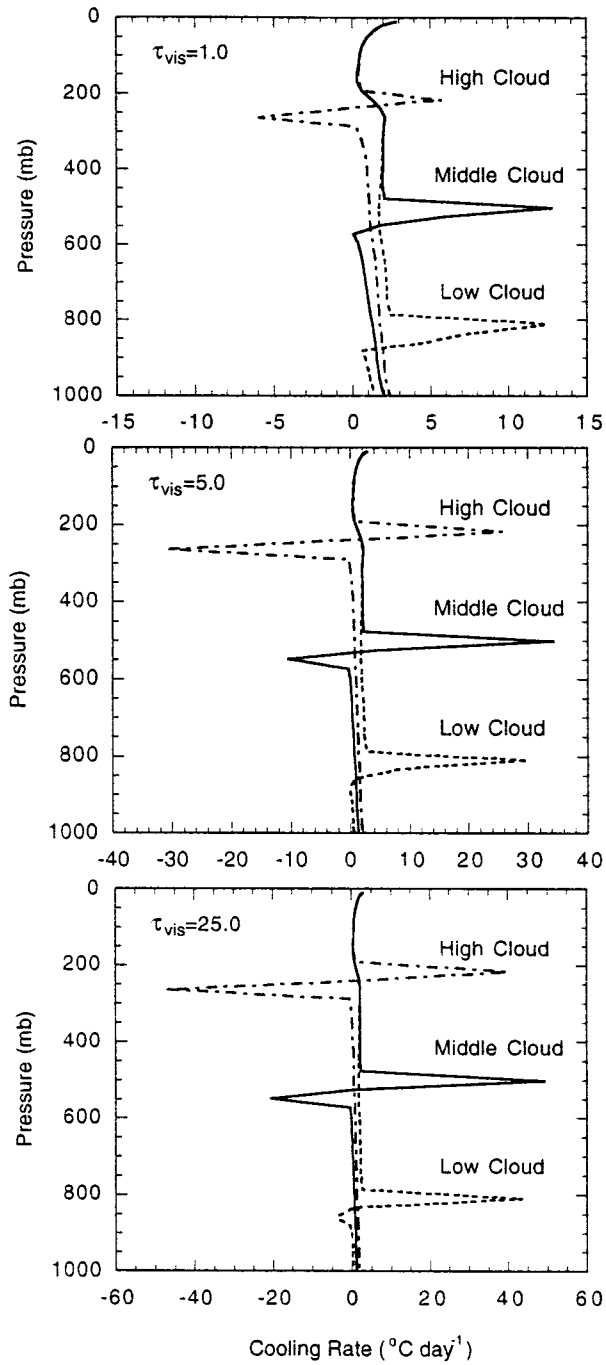

FIG. 8. Cooling rate profiles for the three heights of cloud and three cloud optical thickness in the visible spectral region, τ_{vis}. Scattering by clouds is properly included in the flux calculations by using a six-stream discrete-ordinate scattering algorithm. The midlatitude summer atmosphere is used, $r_w = 50$ μm for the high cloud, and $r_w = 8$ μm for the middle and low clouds

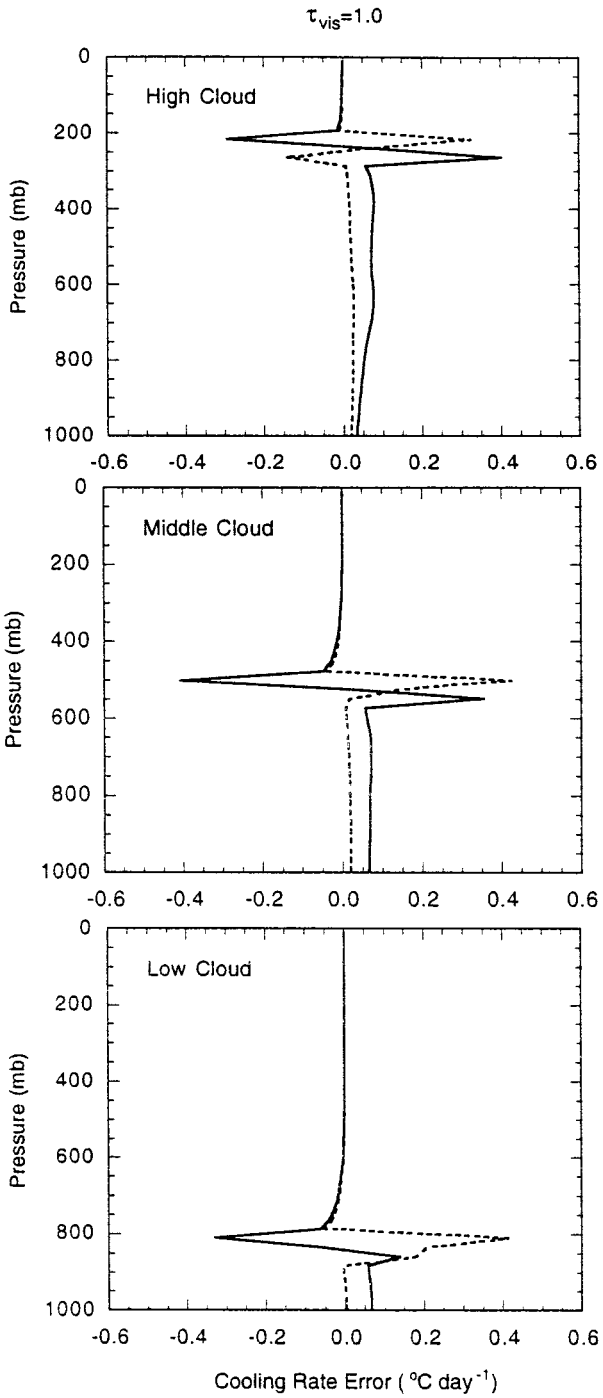

FIG. 9. Cooling rate errors due to the neglect of scattering (solid curves), and the parameterization (dashed curves) for $\tau_{vis} = 1$. The effective cloud particle sizes are $r_w = 50$ μm for the high cloud and $r_w = 8$ μm for the middle and low clouds

for each layer. It can be seen that the cloud top has a very strong cooling for all heights of cloud, whereas the cloud base has a varied degree of warming. For high clouds, the cloud-base heating is very strong due to the large temperature difference between the cloud and the surface.

Cooling rate errors due to the neglect of scattering and the parameterization are given in Figs. 9, 10, and 11 for $\tau_{vis} = 1$, 5, and 25, respectively. Compared to

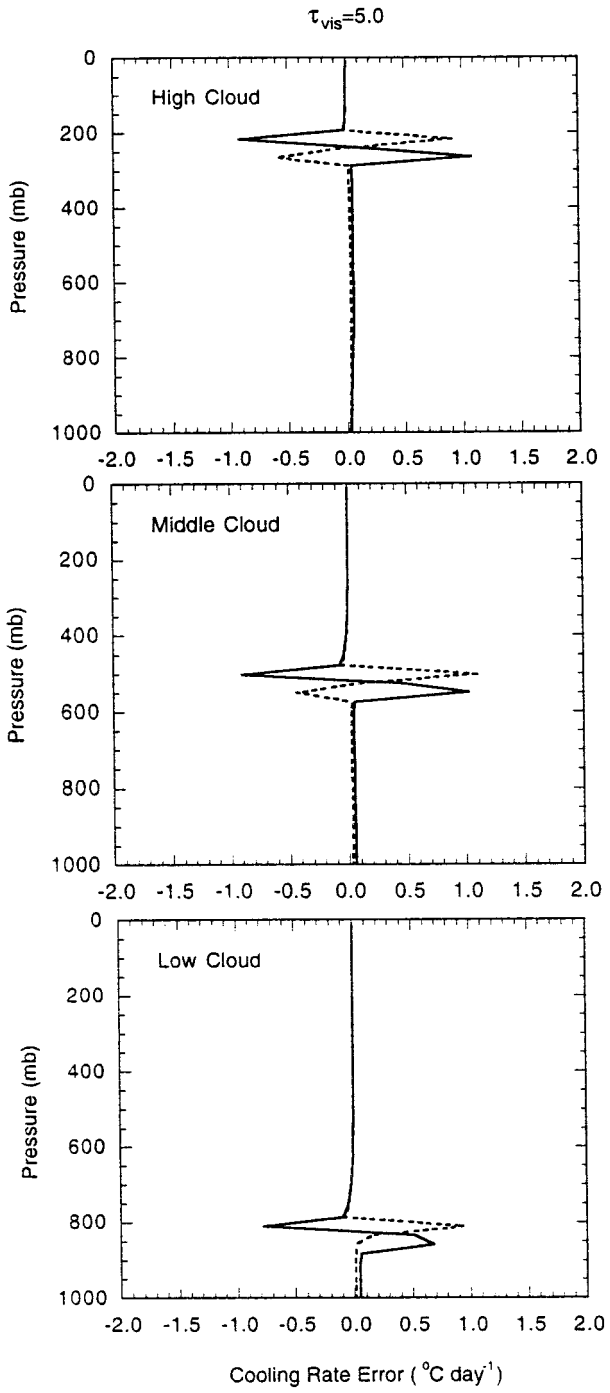

FIG. 10. Same as Fig. 8, except for $\tau_{vis} = 5$.

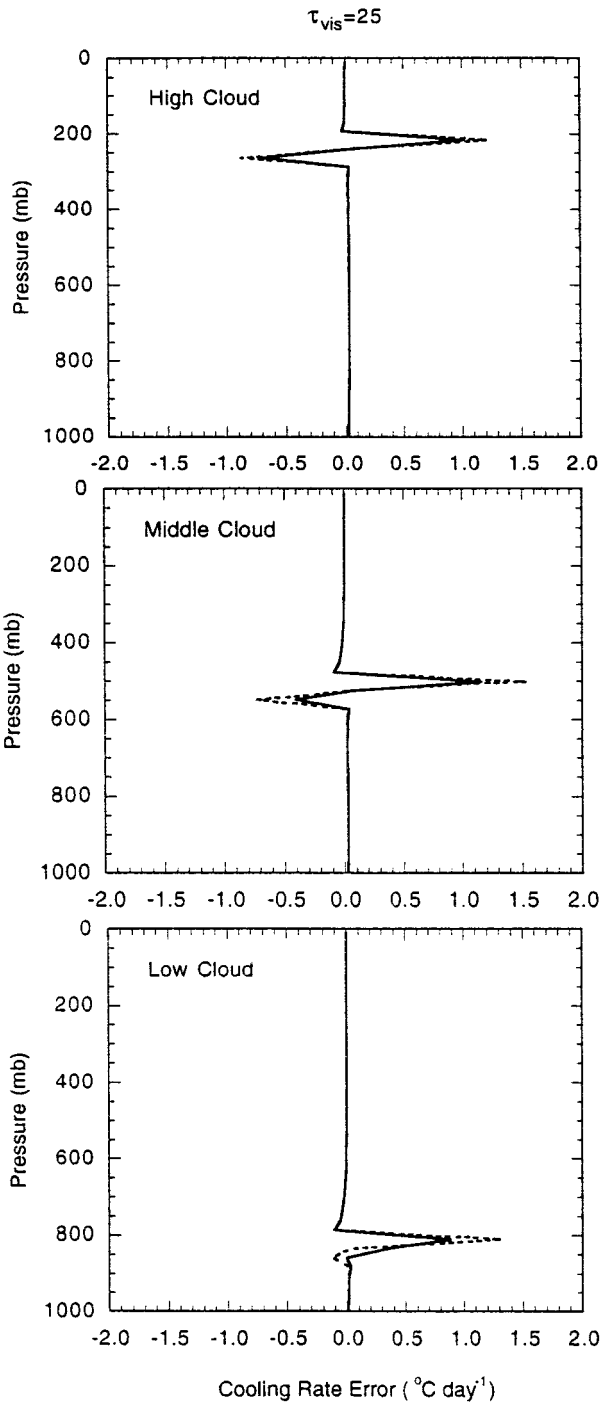

FIG. 11. Same as Fig. 8, except for $\tau_{vis} = 25$.

the cooling rates shown in Fig. 8, the relative error is small. It ranges from 8% for the thin cloud ($\tau_{vis} = 1$) to 3% for the thick cloud ($\tau_{vis} = 25$). The difference in the two approximations decreases with increasing optical thickness. This can be seen from Eqs. (13) and (20) when the scaled optical thicknesses, $\tilde{\tau}$, are both large, and the difference in flux calculations between these two approximations diminishes. The magnitudes of the cooling error in clouds are comparable, but in different signs for $\tau_{vis} = 1$ and 5, between these two approximations. Integrated over the entire atmospheric column, however, the error is much reduced for the parameterization than for the case that scattering is neglected, as can be seen from the flux divergence for the atmospheric column as shown in Figs. 5–7.

5. Implementation in a GCM

Using the discrete-ordinate multiple-scattering algorithm with various streams, Fu et al. (1997) investigated the accuracy and computational efficiency of the approximation that neglected scattering by clouds. Their results show a high accuracy for the two-stream and the combined two- and four-stream approximations when compared with the results using 128 streams. Compared with the case without scattering, the speed for radiative transfer calculations is 4 and 8 times slower for the two-stream and the combined two- and four-stream approximations, respectively. When the total computing time, which also includes computations other than radiative transfer, such as interpolations of the absorption coefficient, calculations of the Planck function and cloud single-scattering properties, etc., the difference in computing time between the no-scattering approximation and the two-stream approximation is reduced to 20%.

While the accuracy of either the two-stream approximation or the combined two- and four stream approximation is accurate and does not impose much computational burden, these discrete-ordinate scattering algorithms can only apply to plane-parallel atmospheres. A commonly used approach to applying these algorithms to an atmosphere where some of the layers are filled partly with clouds, as in most climate models, is to smear (or scale) the cloud optical thickness of a partly cloudy layer over the entire layer in such a way that the reflectance of the layer is the same as that of a partly cloudy layer. The scaling of cloud optical thickness should be a function of the fractional cover and the cloud optical thickness itself (Chou et al. 1998). In principle, it should also depend on the overlapping of clouds at different heights. This approach will certainly introduce uncertainty in flux calculations. Another more straightforward approach is to divide the atmosphere into sections wherein a layer is either cloud-free or totally cloudy. Depending upon the number of cloud layers and the assumption applied to the overlapping of clouds in different layers, computational burden of this approach could be insurmountable.

With the scaling of the optical thickness using (13), clouds are treated as if there were no scattering, and the efficiency of radiative transfer calculations in a partly cloudy atmosphere is nearly identical in a clear atmosphere. As an example, we demonstrate here how this parameterization is implemented in the GEOS GCM (Schubert et al. 1993). A random-maximum assumption is applied for the overlapping of clouds at different heights (Fig. 12). Clouds are grouped into three heights: high, middle, and low approximately separated by the 400-mb and 700-mb levels. Clouds are assumed maximally overlapped within each group and randomly overlapped among different groups. These assumptions are based on the reasoning that neighboring cloud layers are highly connected and distant layers are likely decoupled. With the scaling of (13) for the optical thickness and the random-maximum assumption for cloud overlapping, the transmittance between any two levels are computed according to the following steps:

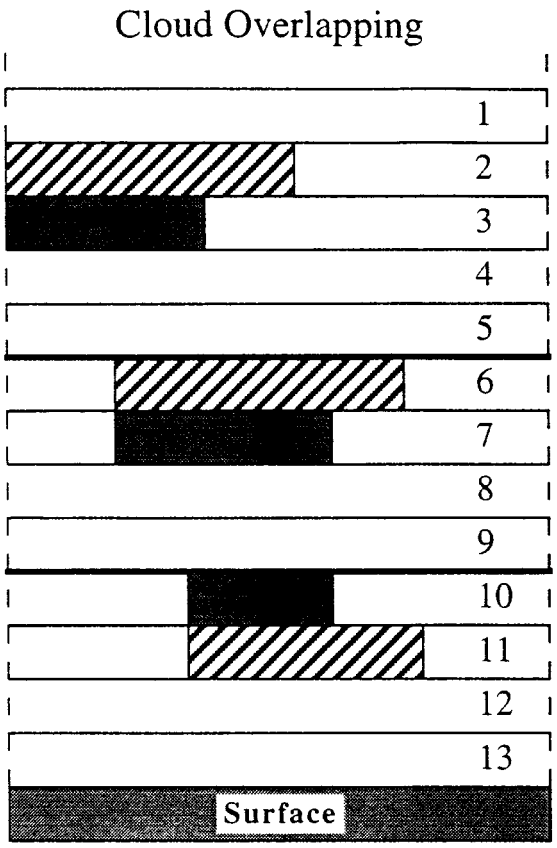

FIG. 12. The random-maximum assumption used for the overlapping of clouds at different heights.

1) A nonopaque cloud layer, l, with a fractional cover A is reduced to an opaque cloud layer with a fractional cover N according to (cf. Chou and Suarez 1994)

$$N_l = A_l(1 - e^{-1.66\tilde{\tau}_l}), \tag{24}$$

so that the transmittances of a layer before and after the scaling are the same, where $\tilde{\tau}$ and N are spectral-band dependent.

2) For a given pair of pressure levels, i and j, the effective fractional cover for each height group, I, is computed using the maximum overlapping assumption,

$$N^I = \max(N_m, \ldots, N_n), \qquad I = 1, 2, 3, \tag{25}$$

where $m, \ldots, n$ are indices for layers between the levels i and j and within the height group I.

3) Using the random overlapping assumptions among height groups, the clear line of sight between the levels i and j is computed from (cf. Harshvardhan et al. 1987)

$$1 - N = (1 - N^1)(1 - N^2)(1 - N^3), \tag{26}$$

where $N^I = 0$ if both pressure levels i and j are outside the height group I.

4) Flux transmittance between the levels i and j is computed from

$$T(p_i, p_j) = (1 - N)T_{\text{clr}}(p_i, p_j), \quad (27)$$

where T_{clr} is the flux transmittance of clear skies. Finally, fluxes are computed from (17) and (19) without requiring the use of multiple-scattering algorithms.

6. Conclusions

Almost without exception, the effect of scattering of thermal IR radiation by clouds is ignored in climate studies for two reasons: 1) Absorption due to water vapor and clouds is strong, and scattering is of secondary importance. 2) It is difficult to implement a multiple-scattering algorithm in a LW radiation routine because of a large amount of computing time required. In this study, we use the LW radiation scheme of Chou et al. (1993) and the discrete-ordinate multiple-scattering algorithm of Stamnes et al. (1988) to investigate the effect of the scattering of LW radiation by clouds and to develop a simple yet effective parameterization for the LW scattering by clouds. For widely different atmospheric conditions, different cloud heights, and large ranges of the cloud optical thickness and particle size, the effect of the scattering of LW radiation by clouds is found to be non-negligible. The effect on the LW flux at the top of the atmosphere exceeds $+8$ W m^{-2} for high clouds when the optical thickness in the visible spectral region, τ_{vis}, is 2–3. The maximum effect on the surface flux is ≈ -4 W m^{-2} for low clouds and also occurs at $\tau_{\text{vis}} \approx$ 2–3.

To parameterize the effect of scattering by clouds, the optical thickness is scaled by a function of the single-scattering albedo and asymmetry factor, which is derived by including the backward-scattering in the emission of a layer and in the transmission between levels. With the parameterization, the flux error is reduced to ≈ 4 W m^{-2} at the top of the atmosphere and to ≈ 2 W m^{-2} at the surface. These errors vary only slightly with the cloud optical thickness. The radiative transfer equations for the parameterization are identical with those for nonscattering atmospheres, and so is the computing time. The parameterization is, therefore, suitable for use in GCM climate studies. There are many sources of uncertianty in flux and cooling rate calculations in both clear and cloudy atmospheres. Our study represents an effort to reduce one source of systematic errors in LW flux calculations.

Acknowledgments. The work of M.-D. Chou was supported by the Global Atmospheric Modeling and Analysis Program, NASA/Office of Earth Science.

REFERENCES

Anderson, G. P., S. A. Clough, F. X. Kneizys, J. H. Chetwynd, and E. P. Shettle, 1986: AFGL atmospheric constituent profiles (0–120 km). AFGL-TR-86-0110, 43 pp. [NTIS ADA175173.]

Cahalan, R. F., W. Ridgway, W. J. Wiscombe, and T. L. Bell, 1994: The albedo of stratocumulus clouds. *J. Atmos. Sci.,* **51,** 2434–2455.

Chou, M.-D., and M. J. Suarez, 1994: An efficient thermal infrared radiation parameterization for use in general circulation models. NASA Tech. Memo. 104606, Vol. 3, 85 pp. [NTIS N95-15745.]

——, W. Ridgway, and M. M.-H. Yan, 1993: One-parameter scaling and exponential-sum fitting for water vapor and CO_2 infrared transmission functions. *J. Atmos. Sci.,* **50,** 2294–2303.

——, M. J. Suarez, C.-H. Ho, M. M.-H. Yan, and K. T. Lee, 1998: Parameterizations for cloud overlapping and shortwave single-scattering properties for use in general circulation and cloud ensemble models. *J. Climate,* **11,** 201–214.

Fu, Q., 1996: An accurate parameterization of the solar radiative properties of cirrus clouds for climate models. *J. Climate,* **9,** 2058–2082.

——, K.-N. Liou, M. C. Cribb, T. P. Charlock, and A. Grossman, 1997: Multiple scattering parameterization in thermal infrared radiative transfer. *J. Atmos. Sci.,* **54,** 2799–2812.

——, P. Yang, and W. B. Sun, 1998: An accurate parameterization of the infrared radiative properties of cirrus clouds for climate models. *J. Climate,* **11,** 2223–2237.

Harshvardhan, and J. A. Weinman, 1982: Infrared radiative transfer through a regular array of cuboidal clouds. *J. Atmos. Sci.,* **39,** 431–439.

——, D. A. Randall, and T. G. Corsetti, 1987: A fast radiation parameterization for atmospheric circulation models. *J. Geophys. Res.,* **92,** 1009–1016.

Killen, R. M., and R. G. Ellingson, 1994: The effect of shape and spatial distribution of cumulus clouds on longwave irradiance. *J. Atmos. Sci.,* **51,** 2123–2136.

O'Brien, D. M., L. J. Rikus, A. C. Dilley, and M. Edwards, 1997: Spectral analysis of infrared heating in clouds computed with two-stream radiation codes. *J. Quant. Spectrosc. Radiat. Transfer,* **57,** 725–737.

Schubert, S. D., R. B. Rood, and J. Pfaendtner, 1993: An assimilated dataset for earth science applications. *Bull. Amer. Meteor. Soc.,* **74,** 2331–2342.

Stamnes, K., S.-C. Tsay, W. Wiscombe, and K. Jayaweera, 1988: Numerically stable algorithm for discrete-ordinate-method radiative transfer in multiple scattering and emitting layered media. *Appl. Opt.,* **27,** 2502–2509.

Tao, W.-K., S. Long, J. Simpson, C.-H. Sui, B. Ferrier, and M.-D. Chou, 1996: Cloud-radiation mechanisms associated with a tropical and a mid-latitude squall line. *J. Atmos. Sci.,* **53,** 2624–2651.